



Share Your Innovations through JACS Directory

# Journal of Nanoscience and Technology

Visit Journal at <http://www.jacsdirectory.com/jnst>

## Synthesis and Structural Characteristics of Fe Doped ZnO Nanoparticles at Different Molarities and Temperatures

Anup Kr Kalita, Sanjib Karmakar\*

Department of Instrumentation and USIC, Gauhati University, Guwahati – 781 014, Assam, India.

### ARTICLE DETAILS

#### Article history:

Received 04 March 2019

Accepted 30 March 2019

Available online 30 April 2019

#### Keywords:

X-Ray Diffraction

Microstrain

Uniform Deformation Model (UDM)

### ABSTRACT

Iron doped zinc oxide (Fe:ZnO) nanoparticles are prepared by wet chemical method at different molarities (0.025 M, 0.05 M and 0.1 M) and different temperatures (RT and 473 K). The nanoparticles are studied by X-ray diffraction (XRD), transmission electron microscopy (TEM) techniques. Crystallite sizes and lattice strain of nanoparticles are calculated by Williamson Hall (W-H) method. The average particle size of the nanoparticle is also calculated by Scherrer formula. Uniform deformation model (UDM), uniform stress deformation model (USDM) and uniform deformation energy density model (UDEM) are used to calculate stress, strain, and energy density involved in the sample. We get different particle sizes of nano particle perpendicular to different (hkl) planes. This shows that particles are not spherical in nature, particles are like rectangular block. It has been also observed from transmission electron micrograph that particles are of rectangular block types. The annealed sample shows larger particle size compared to the sample prepared at room temperature, which is an input for band gap engineering studies.

### 1. Introduction

The nanoscale system and the special properties of the material in this range have attracted people throughout the world [1]. Due to the reduction in size, the particles in the nanometric range show different structural, mechanical, electronic and optical properties which are quite different from those of the corresponding bulk materials [2]. Due to Quantum size confinement, these nano materials due to their peculiar characteristics often show novel physical properties compared to those of the bulk counterpart. If the size and shape of these particles can be controlled, it will be possible to enhance the properties of the material and device function beyond the already established ones. Therefore, large amount of works on syntheses, characterization and fabrication of device are going on worldwide. ZnO is a semiconductor crystal with 60meV binding energy and wide band gap of 3.3 eV at room temperature (RT) [3]. It is also important due to its range of optical and electrical properties. The ZnO nanoparticles are used in variety of applications such as Solar cell [4], UV light emitters [5], Light emitting diodes [6] and in many other industrial purpose. Out of all the methods for the fabrication of nanoparticle, we have applied wet chemical method [7-9], which is the most cost effective for large scale production.

### 2. Experimental Methods

#### 2.1 Instrumentation

The average particle size is calculated from X-ray diffraction pattern. The phase and the structure of ZnO nanoparticles are studied from the diffractogram obtained from X-ray diffractometer (X' Pert Pro). The diffractometer is set with generator setting of 30 mA and 40 kV with  $\text{CuK}\alpha_1$  ( $\lambda=1.54056 \text{ \AA}$ ) radiation. The XRD is calibrated with a standard silicon sample. The broadening of peaks is corrected with Warren rule [10-12] that arises due to instrumental effect. Continuous scanning is applied in the range from 25-90° (2 $\theta$ ) at a scanning rate of 1 sec/step and step size is 0.02° of 2 $\theta$ . The HRTEM (TEM, Jeol JEM 2100 200 kV) image of the ZnO nanoparticle at annealed temperature give the size and morphology of the

ZnO nanoparticle. The optical absorption spectra of ZnO are recorded by a UV-Vis spectrometer (HITACHI model U-3210).

#### 2.2 Chemicals

Materials with highest purity (99.99%) were purchased. Zinc acetate dihydrate ( $\text{CH}_3\text{COO}_2\text{Zn}\cdot 2\text{H}_2\text{O}$ ) and sodium hydroxide (NaOH) as the starting materials, polyvinyl alcohol (PVA) as capping agent and double distilled water as dispersing solvent are used to prepare the ZnO thin film.

#### 2.3 Preparation of ZnO Nanoparticle in Thin Films

In the experimental process the 0.1 M, 0.05 M and 0.025 M solution of zinc acetate dihydrate ( $\text{CH}_3\text{COO}_2\text{Zn}\cdot 2\text{H}_2\text{O}$ ) are stirred constantly for 1 hour at 343 K (solution 1, 2, 3). PVA is stirred constantly at 343 K (solution 4, 5, 6) to prepare 0.1 M, 0.05 M and 0.025 M solution. Now NaOH is slowly added drop by drop into the (solution 1, 2, 3) and stirred at room temperature for half an hour and white solutions is obtained as (solution 7, 8, 9). Again, to prepare iron (Fe) doped ZnO we prepared  $\text{FeCl}_3$  solution separately of three different concentration 0.025 M, 0.05 M and 0.1 M as (solution 10, 11, 12) and mixed with the solution of (4, 5, 6) and (7, 8, 9) to have solution (13, 14, 15). The thin films are deposited on glass substrate. Therefore, Glass substrates are washed perfectly with some acid and then with distilled water and allowed to dry at room temperature. The substrates are dipped into the final solution (13, 14, 15) for 24 hours. After 24 hours the glass substrates are removed from solutions (13, 14, 15) and allowed to dry at room temperature. The experiment is done for as deposited and annealed films. The sample is annealed in order to improve the film crystallinity as well as to clean the surface from probable absorbed impurities [13].

### 3. Results and Discussion

#### 3.1 X-Ray Diffraction Analysis

Figs. 1 and 2 represent the X-ray diffraction pattern of 0.025 M, 0.05 M and 0.1 M iron doped ZnO nanoparticle at room temperature and annealed at 473 K individually. From the graphs it is observed that the grown films are polycrystalline in nature. The diffraction peak of nanoparticles for 0.025 M at room temperature corresponds to (100), (002), (101), (101), (102), (110), (112) lattice plane, diffraction peaks for 0.05 M at room temperature corresponds to (100), (002), (101), (102), (110), (103), (112)

\*Corresponding Author: sanjibkab@rediffmail.com (Sanjib Karmakar)

lattice planes, and diffraction peaks for 0.1 M at room temperature corresponds to (100), (002), (101), (102), (110), (103), (112) lattice planes. Due to annealing at 473 K diffraction peaks for 0.025 M corresponds to the lattice planes (100), (002), (101), (102), (110), (112) diffraction peaks for 0.05 M corresponds to the lattice planes (100), (002), (101), (102), (110), (103), (112), (201) and diffraction peaks for 0.1 M corresponds to the lattice planes (100), (002), (101), (102), (110), (103), (112), (201) planes that are almost matched with standard ZnO powder (ICDD No. 80-0074). The peak intensity has increased with increase in molarity at both temperatures. The standard ZnO powder is crystallized in a hexagonal system with  $a = 3.2535$ ,  $c = 5.2151$  and space group is  $P6_3mc$  (186). We have found the lattice parameters 'a' = 3.2543, 3.2452, 3.2456 and 'c' = 5.2163, 5.2175, 5.2134 at 0.025 M, 0.05 M and 0.1 M for nanoparticles prepared at RT and 473 K respectively.

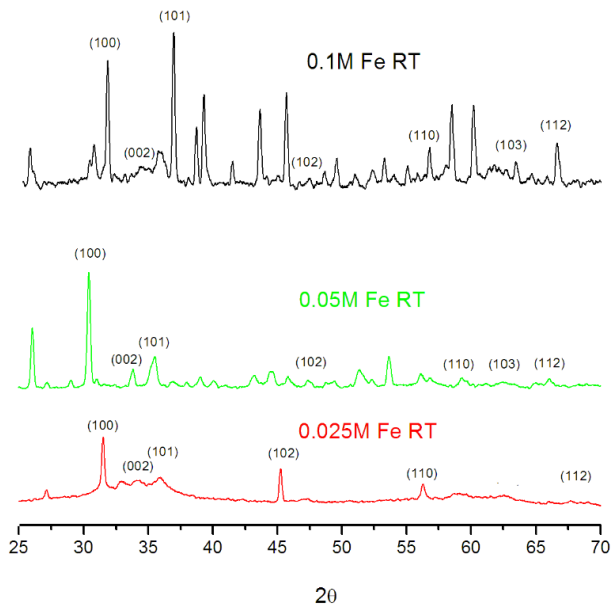


Fig. 1 XRD diffraction pattern of 0.025 M, 0.05 M and 0.1 M Fe doped ZnO at RT

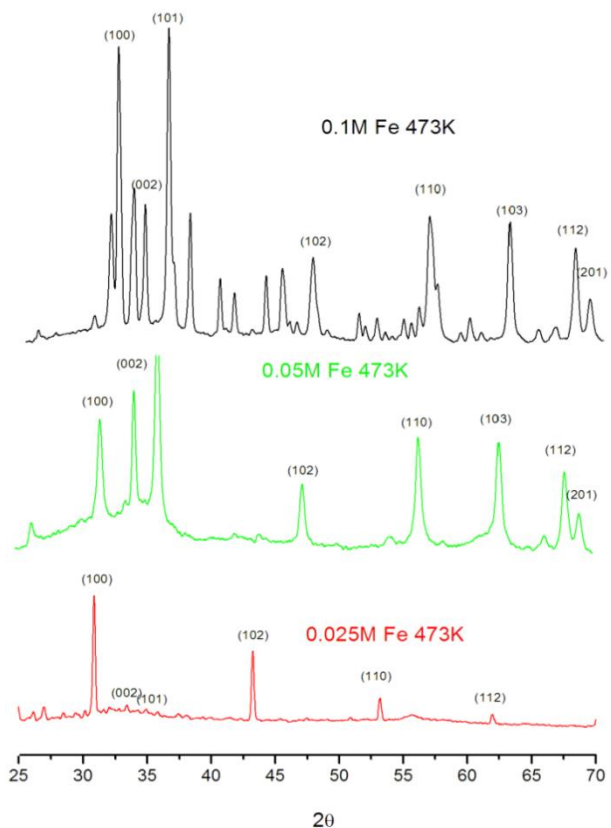


Fig. 2 XRD diffraction pattern of 0.025 M, 0.05 M and 0.1 M Fe doped ZnO at 473 K

Due to shifts of the diffraction peaks the small changes are observed in the length of the lattice axes of the prepared nanoparticles. It has been observed that with the increase in concentration the intensity of peaks is

<https://doi.org/10.30799/jnst.213.19050118>

increased from room temperature and at 473 K. This variation in peak intensity directly shows the impact of doping concentration on surface texture of the nanoparticle. The intensity of various diffraction peak are different, which confirms the anisotropic growth of ZnO nanoparticle [14]. At 0.025 M dominant peak is at (100) whereas at 0.05 M the dominant peak is at (101) and at 0.1 M the peak is at (100). There is a small angular positional increment for all the peak positions which indicates the idea of defect development in the nanoparticle. Thus, the crystalline quality has been degraded with increase in doping concentration. Due to annealing the crystalline quality has been improved and it has been observed that there is increase in intensity for the sample of different molarity which suggests that crystalline quality has improved again.

The different results of the above experiment are due to the different distribution of Fe ions on ZnO thin films. This shifting indicates the development of strain or defects in the sample prepared at RT and annealed at 473 K. This small change observed in the length of the lattice axes of the prepared nanoparticles is due to shifts of the diffraction peaks. No diffraction peaks from other species could be observed which indicates that no structural deformation occurred in ZnO lattice due to iron (Fe) doping. It summarizes that Fe has been successfully substituted in Zn lattice sites in ZnO matrix. The sharp peaks indicate that the products are well crystallized. X-ray peak intensities are weak and broad compared to bulk sample of ZnO, suggesting the small crystalline size. The distance between lattice planes (d values) are calculated using Bragg's equation given by,  $\lambda = 2d \sin \theta$ , where  $\lambda$  is wavelength of the X-ray beam, d interplanar spacing and  $\theta$  is the Bragg angle.

It is observed that both peak shift and broadening are present in the peaks of the prepared nanoparticles. The observed shifts in the peaks of the nanoparticles are because of the development of defects in the nanoparticles at higher calcinations temperature. At higher calcinations temperature peaks become more and more intense with reduced broadening, which indicate the increase in grain size with increasing temperature [15]. During this slow heating and subsequent cooling, the crystal grows and results in the increase in particle size [16]. During deformation, the d-spacing for a given (hkl) plane will change (i.e. peak shift) and the associated lattice strain can be calculated. Diffraction peak broaden either because of homogenous micro strain induced by dislocation-like defects (strain broadening) or because of shrinkage of coherent scattering volume (size broadening). The observed broadening of peak is likely the combined result of both effects. Fig. 3 shows the strain extracted from the slopes at RT and annealed at 473 K respectively.

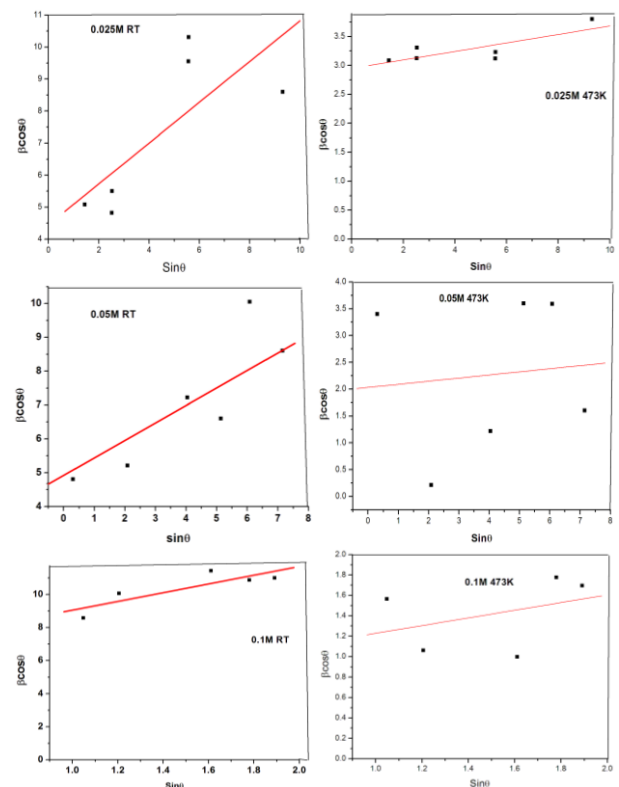


Fig. 3 Williamson Hall plot of iron doped ZnO at 0.025 M, 0.05 M and 0.1 M at RT and 473 K using UDM model

It has been observed that there is non-linearity in the W-H plot, which indicates the presence of strain anisotropy in the prepared sample. Strain broadening and size broadening can be separated from W-H plot in Fig. 3.

ZnO nanostructures may have a number of defects such as oxygen vacancies, lattice disorders, etc. Due to annealing the defects are removed and the lattice contracts. Also lattice relaxation due to dangling bonds should be taken into account. The dangling bonds of ZnO surface interact with oxygen ions from the atmosphere and due to electrostatic attraction, leading to a lattice that is slightly contracted [14, 15]. The particle sizes are determined for the preferred planes (hkl) using Debye Scherrer formula [17]. The average particle size obtained by using Scherrer formula is shown in Table 1. The particle size and microstrain from W-H plot is shown in Table 2.

**Table 1** Variation of the particle size at Room Temperature and 473 K for 0.025 M, 0.05 M and 0.1 M Fe doping

Temperature	0.025 M	0.05 M	0.1 M
RT	18 nm	20.4 nm	22.6 nm
473 K	27.11 nm	27.23 nm	33.3 nm

**Table 2** Variation of the particle size and microstrain obtained from W-H plot at room temperature and 473 K for 0.025 M, 0.05 M and 0.1 M Fe doping

Molarity	Temperature	Particle size	Microstrain
0.025 M	RT	34.2 nm	0.0612
	473 K	55 nm	0.0046
0.05 M	RT	33.4 nm	0.0722
	473 K	66 nm	0.0293
0.1 M	RT	18 nm	0.0877
	473 K	22 nm	0.0023

Scherrer method gives average particle size of all crystallites present in the sample in a direction perpendicular to a particular (hkl) planes. And W-H method gives the average particle size in all directions of all individual particles. As the Scherrer method and W-H method give almost equal average particle size, this is possible only if the shape of the particles is cubical or spherical.

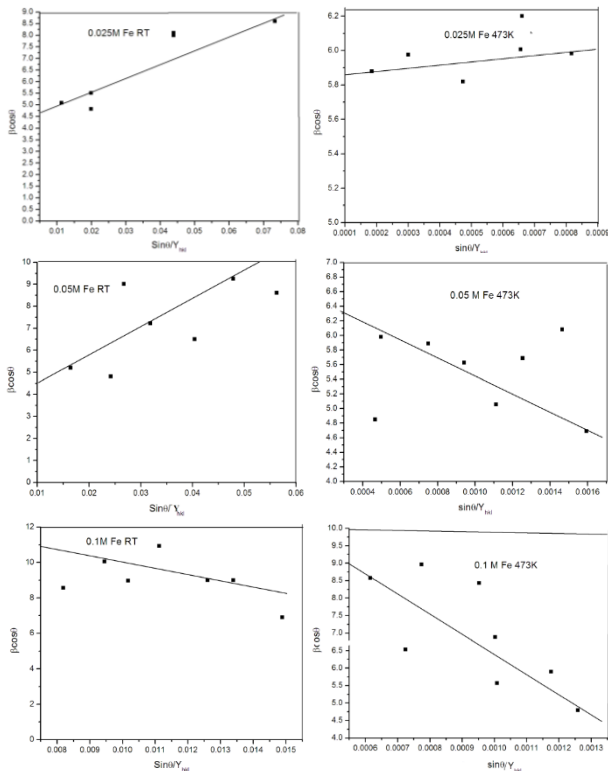


**Fig. 4** Williamson Hall plot of Iron doped ZnO at 0.025 M, 0.05 M and 0.1 M at RT and 473 K using USDM model

XRD line broadening arises due to small grain size and strain. Grain size causes the radiation to be diffracted individually [18]. Using Williamson-Hall plot particle size and microstrain using the equation,  $\beta\cos\theta = m\sin\theta + \lambda/D$ , where  $m'$  is the microstrain,  $D$  is the particle size and  $\beta$  is the full width at half maximum of the peak measured in radian,  $2\theta$  is the diffraction angle and  $\lambda$  is the wavelength of X-ray. The slope of  $\beta\cos\theta$  vs  $\sin^2\theta$  graph gives the strain in the particle and the intercept on Y axis give  $\lambda/D$ . Fig. 4 shows the Williamson-Hall plot of the ZnO nanoparticle annealed at RT and 473 K respectively. From Scherrer Equation as well as from W-H (UDM) plot it has been observed that the particle size increases <https://doi.org/10.30799/jnst.213.19050118>

as the substrate temperature increases and strain decreases with the increase in annealing temperature.

Uniform Stress Deformation Model (USDM) is also used to calculate strain [20, 21] from Hooke's law  $\sigma = Ye$ , where  $\sigma$  give stress,  $Y$  Young's modulus of elasticity. This equation is valid for small amount of strain.

For hexagonal crystal, Young's modulus is given by,

$$Y_{hkl} = E_{hkl} \frac{[h^2 + \frac{(h+2k)^2}{3} + (\frac{a^2l^2}{c^2})]^2}{s_{11}(h^2 + \frac{(h+2k)^2}{3})^2 + s_{33}\frac{a^4l^4}{c^4} + (2s_{13} + s_{44})\{h^2 + \frac{(h+2k)^2}{3}\}(\frac{a^2l^2}{c^2})}$$

where  $S_{11}, S_{33}, S_{13}, S_{44}$  be the elastic compliances of ZnO with values  $7.858 \times 10^{-12}, 6.940 \times 10^{-12}, -2.206 \times 10^{-12}$  and  $23.57 \times 10^{-12} \text{ m}^2\text{N}^{-1}$  respectively. Modulus of elasticity of ZnO is approximately 127 GPa. The USDM plot for Fe doped ZnO at different molarity is shown in Fig. 4.

These graph shows the modified form of W-H analysis assuming USDM for iron (Fe) doped ZnO. The slope gives the stress and the crystal size is calculated from the intercept on Y axis. The energy density of a crystal is calculated from the uniform deformation energy density model (UDEM).

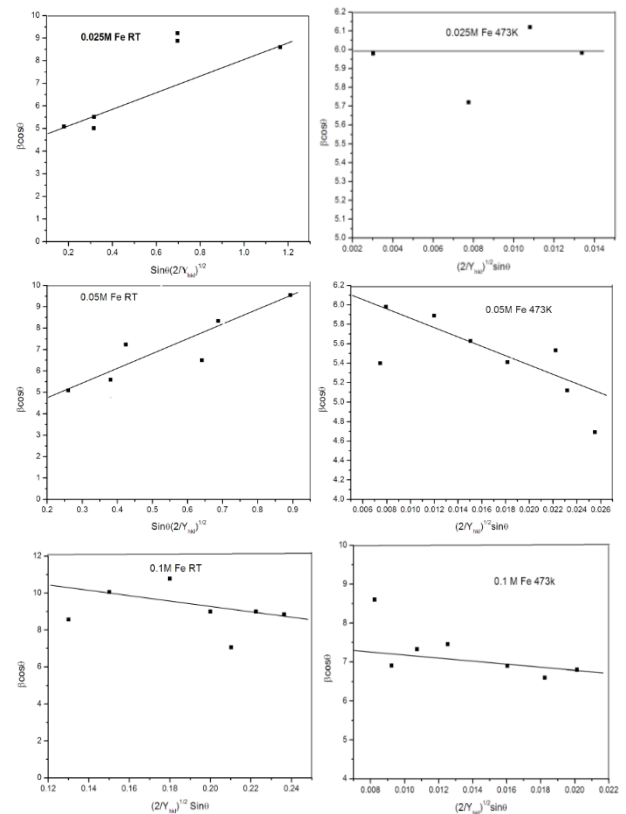


**Fig. 5** Williamson Hall plot of Iron doped ZnO at 0.025 M, 0.05 M and 0.1 M at RT and 473 K using USDM model

These graphs show the modified form of W-H analysis assuming UDEM for iron (Fe) doped ZnO. The slope gives the density of energy and the crystal size is calculated from the intercept on Y axis. The geometric parameters of Iron (Fe) doped ZnO nanoparticles calculated from UDM, USDM and UDEM are shown in the Table 3.

**Table 3** particle size (D), strain (ε), stress(σ) and energy density (u) for prepared Fe doped ZnO nanoparticle at RT and 473K using different methods

Conc.	Temp.	UDM			UDEM					
		D (nm)	ε	σ (Mpa)	D (nm)	ε	σ (Mpa)	u (kJm <sup>-3</sup> )		
0.025 M	RT	34.2	0.0612	30	0.0183	2.34	30.7	0.0136	1.78	0.0121
	473 K	55	0.0046	37.9	0.0113	1.70	38.8	0.0113	1.48	0.0082
0.05 M	RT	33.4	0.0722	29.7	0.0311	3.98	30.8	0.0016	0.22	0.0003
	473 K	66	0.0293	41.0	0.0120	1.56	39.6	0.0056	0.79	0.0022
0.1 M	RT	18	0.0877	58.8	0.0110	1.41	70	0.0096	1.27	0.0064
	473 K	22	0.0233	69.2	0.0596	7.62	73.1	0.046	6.02	0.1383

**3.2 TEM Study**

The HRTEM (TEM, Jeol JEM 2100 200kV) images of the ZnO nanoparticle at annealed temperature are taken. The size and morphology of the ZnO nanoparticle were investigated through TEM micrograph. Image reveals that the average particle size is about 25-35 nm which is in good agreement with that estimated by Scherrer formula.

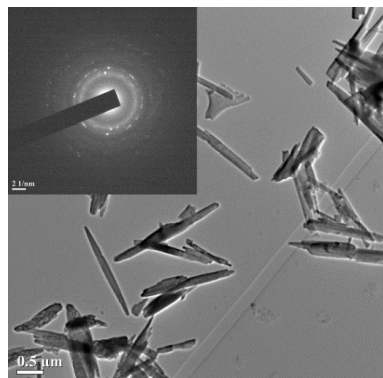


Fig. 6 HRTEM image with SAED pattern of Fe doped ZnO

#### 4. Conclusion

ZnO nanoparticles have been prepared using wet chemical syntheses method and were characterized by XRD and TEM characterizations. XRD and TEM confirm the nanostructure for the prepared ZnO nanoparticles. SAED pattern consists of bright uniform rings which reveals that the as prepared samples are polycrystalline in nature. The significant sharp absorption of UV radiation by ZnO nanoparticles indicates the monodispersed nature of the nanoparticle distribution. UDM, USDM and UDEDM method give stress, strain and energy density involved in the sample. The result obtained from UDM, USDM and UDEDM approximation of W-H plot predict different values of crystallite size and lattice strain. These ZnO nanoparticles can be used in different applications like sensors, active medium for lasers etc.

#### Acknowledgement

We thank SAIF, Department of Instrumentation and USIC, Gauhati University, Guwahati – 781 014 for providing X-ray diffraction pattern and SAIF, NEHU, Shillong for providing the HRTEM image.

#### References

- [1] S. Basri, M. Sarjidan, W. Majid, Structural and optical properties of nickel-doped and undoped zinc oxide thin films deposited by sol-gel method, *Adv. Mater. Res.* 895 (2014) 250-256.
- [2] P. Kalita, B.K. Sharma, H.L. Das, Structural characterization of vacuum evaporated ZnSe thin films, *Bull. Mater. Sci.* 23 (2000) 313-317.
- [3] M.K. Debnath, S. Karmakar, Study of blue shift of optical band gap in zinc oxide (ZnO) nanoparticles prepared by low-temperature wet chemical method, *Mater. Lett.* 111 (2013) 116-119.
- [4] A. Yadav, Virendra Prasad, A.A. Kathe, Sheela Raj, Deepty Yadav, et al., Functional finishing in cotton using zinc oxide nanoparticles, *Bull. Mater. Sci.* 29 (2006) 641-645.
- [5] Jiwei Zhai, Hayden Chen, Direct current field and temperature dependent behavior of antiferroelectric to ferroelectric switching in highly (100) - oriented PbZrO<sub>3</sub> thin films, *Appl. Phys. Lett.* 82 (2003) 2673-2679.
- [6] Qinyi Zhang, Changsheng Xie, Shunping Zhang, Aihua Wang, B. Zhu, et al., Identification and pattern recognition analysis of Chinese liquors by doped nano ZnO sensor array, *Sensor. Actuator B* 110 (2005) 370-376.
- [7] M. Debnath, S. Karmakar, J. Borah, Structural characterization of ZnO nanoparticles synthesized by wet chemical method, *Adv. Sci. Eng. Med.* 4 (2012) 306-311.
- [8] I.M. Ali, Lattice thermal conductivity and correction term (GaN) compound, *Jour. Basrah Res.* 37 (2011) 1-14.
- [9] A. Verkey, A.F. Fort, Transparent conducting cadmium oxide thin films prepared by solution growth technique, *Thin Solid Films* 239 (1994) 211-213.
- [10] K. Siddique, B. Kumar Nath, Sanjib Karmakar, Study of structural and dielectric properties of copper oxide nanoparticles prepared by wet chemical method, *Int. J. Nanosci.* 12 (2013) 1350036-1350041.
- [11] B.E. Warren, X-ray studies of deformed metals, *Metal Phys.* 8 (1959) 147-202.
- [12] K. Siddique, S. Karmakar, Synthesis and characterization of nickel oxide nanoparticles by PVA matrix method, *Int. J. Manag. IT Eng.* 3 (2013) 586-589.
- [13] L. Alexander, H.P. Klug, Determination of crystallite size with the X-ray spectrometer, *Jour. Appl. Phys.* 21 (1950) 137-141.
- [14] G.K. Williamson, W.H. Hall, X-ray line broadening from field aluminium and wolfram, *Acta Metal.* 1 (1953) 22-31.
- [15] T. Srinivasulu, K.T. Ramakrishna reddy synthesis and charactersation of Fe doped ZnO thin films deposited by chemical spray pyrolysis, *Modern Electron. Mater.* 3(2017) 76-85.
- [16] A. Parra-Palomino, O. Perales-Perez, R. Singhal, M. Tomar, J. Hwang, P.M. Voyles Structural, optical and magnetic characterization of monodisperse Fe-doped ZnO nanocrystals, *J. Appl. Phys.* 103 (2008) 07D121-125.
- [17] A. Gotkas, I.H. Mutlu, Y. Yamada, Influence of iron doping on structural, optical and magnetic properties of ZnO thin films prepared by sol-gel method, *Superlattice Microstruct.* 57 (2013) 139-149.